Geophysica (1996), 32(1-2), 127-165

Stratospheric Ozone Depletion and Solar UV Radiation in the Arctic and Its Potential Impact on Human Health in Finland

P. Taalas[1], E. Kyrö[2], K. Jokela[3], T. Koskela[1], K. Leszczynski[3], M. Rummukainen[2], J. Damski[1] and Ari Supperi[1]

[1] Finnish Meteorological Institute (FMI), Meteorological Research/Ozone and UV Research, Helsinki, Finland

[2] Finnish Meteorological Institute, Sodankylä Observatory, Sodankylä, Finland

[3] Finnish Centre for Radiation and Nuclear Safety (STUK), Non-Ionising Radiation Laboratory, Helsinki, Finland

(Received: December 1995; Accepted: October 1996)

Abstract

A Finnish national climate research programme, SILMU, has funded three projects in the field of ozone and UV radiation research during 1990-1995. The results of these projects are summarised here. The study of temperature sounding records made in Finland 1958-94 has revealed a warming trend in the lower and middle troposphere (up to 0.3 K/decade) and a cooling of similar order of magnitude in the lower stratosphere. The cooling has been largest in winter leading possibly to more ozone loss-favouring stratospheric climate. Trends of total ozone for 1979-94 at Sodankylä (1979-88 TOMS overpass data, 1988-94 Brewer) have been -8.0 ± 3.4 %/decade for winter, -3.2 ± 1.5%/decade for summer, and -4.1 ± 1.2%/decade for autumn. A study of tropospheric ozone changes for 1989-94 has revealed a negative "trend" of the order of -2 %/year. Indirect indications of chemically induced ozone loss in the Arctic winter/spring have been found, especially in 1995. Large part of the ozone anomalies observed in the Arctic may have different nature than those observed at Antarctica.

Finnish UV radiation research was to a large degree started during the SILMU project including modelling, broadband and spectral UV measurements and methods for calibration and testing of the instruments. The effect of ozone loss on UV doses have been studied. It has been found out that the effect of ozone loss may be detected from the UV observations. It has been estimated from observations and model calculations that cloudiness is absorbing 40 % of the UV radiation on annual mean basis. It has been calculated that snowcover may intensify the UV irradiance considerably especially on a vertical surface, like human face or eyes. It is calculated that a 12 % ozone loss at 60 °N may lead to 17-33 % increase in non-melanoma skin cancers in Finland during next few decades. The future development of stratospheric ozone in the Arctic depends on the success in reduction of the halogenated compound emissions and on climatic change. Increase of atmospheric CO_2 concentration may change stratospheric climate in the Arctic towards ozone-loss favouring direction with increases in UV-B irradiances.

Key words: ozone, UV radiation, polar vortex, skin cancer

1. *Introduction*

The proposal of possible chemical background for the Antarctic ozone "hole" by *Farman et al.* (1985) led to an enhancement of Arctic ozone research activities. Among these Finnish Meteorological Institute started routine total ozone and ozone sounding measurements at Sodankylä (67.4 °N). Although the first solar UV radiation measurements were made during the 1920's in Finland (*Lunelund* and *Holmberg*, 1929; *Lunelund*, 1944), the first attempts for modern UV monitoring were started in 1990. This included routine UV monitoring with a Brewer spectrophotometer and purchasing of Solar Light 500 erythemal radiometers by the FMI. STUK has tested and recalibrated the SL radiometers in laboratory conditions and, in outdoors conditions by using sun as a UV source.

The Finnish ozone and UV monitoring activities have become a part of international activities, especially the EU Environment and Climate Programme's research projects. The main national level effort has been the Finnish Academy's climatic change programme, SILMU 1990-95. This paper summarises the scientific results reached during the SILMU project.

2. *Methods*

2.1 Ozone and related measurements

There has been a lack of continuos long term ozone and stratospheric measurements in the European Arctic. Sodankylä observatory started ozone monitoring with Russian filter ozonometer in 1987, and with Brewer Mk. II spectrophotometer and ozone sondes in 1988. The programme has gradually evolved further and the present monitoring programme of Sodankylä is summarised in Table 1. In 1991 FMI started total ozone measurements at its Jokioinen Observatory by using M-124 ozonometer. In 1994 double monochromator Brewer spectrophotometer (Mk. III) and DigiCora II ozone sounding equipment were installed at Jokioinen.

2.2 Long-term temperature soundings

Finland has a long history of radiosoundings. The first routine radiosoundings were performed at FMI Ilmala observatory (Helsinki) during the 1930's. In 1960 the Ilmala observatory was moved form Helsinki to Jokioinen. Radiosoundings have been performed at Sodankylä since 1949. *Taalas et al.* (1995) have studied the changes in tropospheric and lower stratospheric temperatures at Jokioinen (1961-93) and at Sodankylä (1965-93).

Table 1. Stratospheric monitoring at FMI the Sodankylä (67.4 °N, 26.6 °E) and Jokioinen (60.8 °N, 23.5°E) observatories. The geographical location of the stations is shown in Figure 1.

SPECIES/OBJECTIVE	INSTRUMENTS	RECORD STARTS IN
1. SODANKYLÄ		
Column O_3	Brewer Mk II and SAOZ *) spectrophotometers	1988
Column SO_2	Brewer	1988
Column NO_2	SAOZ	1990
Column OClO	SAOZ	1995
Vertical distribution of O_3	ECC sondes, Umkehr, microwave radiometer	1988
Vertical distribution of aerosols	Sondes and lidars **)	1994
Solar UV radiation	Brewer and SL500/501 radiometers	1990
Radiosoundings (pTU)	Vaisala radiosondes	1949
2. JOKIOINEN		
Column O_3	Brewer Mk III spectrophotometer	1994
Column SO_2	Brewer	1994
Vertical distribution of O_3	ECC sondes ***), Umkehr	1994
Solar UV radiation	Brewer and SL500/501 radiometers	1991
Radiosoundings (pTU)	Vaisala radiosondes	1960

*) Co-operation between CNRS and FMI

**) Lidar records from winters 1991/92 and 1994/95. New installation within EU SAONAS project in 1996.

***) Ozone soundings during campaigns, like SESAME 1994/95.

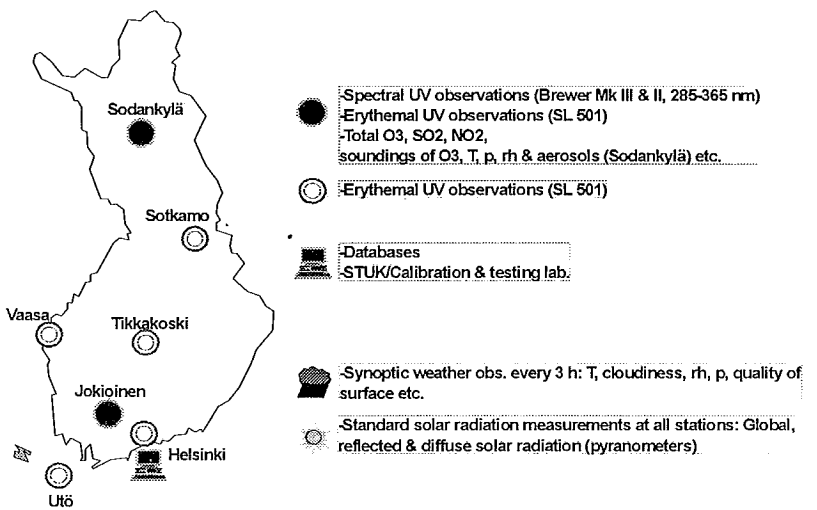

Fig. 1. The location of FMI ozone and UV radiation stations.

The oldest sounding records of Sodankylä before 1965 have recently been digitised. During 1949-57 soundings were performed three hours later in the day than the present sounding times at 00 and 12 UTC and the trends here have been estimated only back to 1958. Changes in instrumentation (e.g. there has been four types of radiosondes in use during the examined period) may cause discontinuities in the time series as seen in Fig. 2. Each change is connected to faster and smaller temperature sensors and if not accounted artificial cooling "trend" may be introduced in the troposphere where temperature increases rapidly with height (*Gaffen*, 1994). In the fairly isothermal stratosphere the lag error is insignificant.

The lag coefficient of a temperature sensor at a pressure level is a function of lag coefficient at the ground level, the air density and the rate of ascent. The lag error is a function of the lag coefficient and the lapse rate of temperature. The error at different pressure levels can be computed by numerical integration from the temperature profile. The measured temperatures are used as initial values for computing the error and the corrected temperatures are used in successive iterations until the lag error becomes smaller than given tolerance. This method was applied to monthly mean temperatures at the main pressure levels for years 1958-1994. The ascent rate used in the calculations was 5.78 m/s, which is the average for the years 1965-1994. The sensor characteristics documented by *Huovila* and *Tuominen*, (1990) have been used in the calculations.

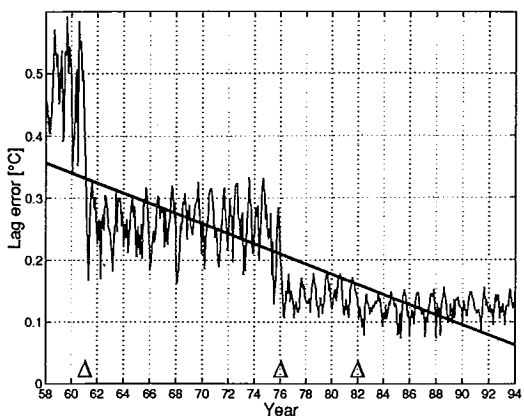

Fig. 2. Lag error of various temperature sensors at 300 hPa level and the "instrumental trend" caused by changes of sensor time coefficients. The triangles indicate the dates of changes of temperature sensors, short experimental periods are excluded.

2.3 Broad-band UV measurements

FMI has installed three Solar Light 500 erythemal radiometers during 1991-92 to Jokioinen, Tikkakoski and Sodankylä (see Fig. 1). These broadband instruments are most sensitive in the UV-B part of solar spectra. Temperature stabilising and defrosting units were built by FMI. In 1995 seven FMI stations were equipped with SL501 radiometers (new stations Helsinki, Utö, Vaasa and Sotkamo). Global, diffuse and reflected solar radiation measurements, as well at least synoptic weather observations are performed at all of the stations. Radiosoundings (pressure, temperature, humidity and winds) are performed at Jokioinen, Tikkakoski and Sodankylä as well as ozone related measurements as shown in Table 1.

To achieve the maximum accuracy and long term stability, the broadband solar UV monitoring instruments have been tested and calibrated by STUK. The calibration is based on comparison with a precision spectroradiometer Optronic 742 (denoted OL 742) by using solar radiation as an UV source. The OL 742 is frequently calibrated against 1000 W quartz-halogen lamps traceable to NIST and PTB.

The reference spectroradiometer and the broadband radiometers have been characterised by measuring spectral responsivities, angular responses temperature sensitivities and slit functions (*Leszczynski et al.*, 1993; *Leszczynski*, 1996; *Leszczynski et al.*, 1996). By applying numerical correction based on the test results an uncertainty level of ± 8% (2 σ) has been achieved for spectral solar UV measurements (*Leszczynski*, 1996). The overall uncertainty is obtained by calculating the square root of the sum of the squares of the sources of uncertainty. The error budget is presented in Table 2.

Table 2. The uncertainty (2 sigma) of the CIE-weighted (*McKinley* and *Diffey*, 1987) solar UV irradiance measurements with the OL 742 spectroradiometer.

Source of uncertainty	Uncertainty (%)
Calibration	
lamp	± 2
alignment	± 3
Measurements	
shift of the wavelength scale	± 3
cosine response	± 5
azimuth response	± 1
temperature	± 3
slit function	± 2
stray light	< ± 1
non-linearity of the detector	± 1
random error	± 3
Overall uncertainty	±8 %

An example of calibration factors (CF:s) of a broadband solar UV radiometer is shown in Figure 3. During the calibration measurements the optical axis of each instrument is directed towards the zenith, and the CF:s are derived from measurements when the sun is not obstructed with the clouds. The uncertainty of the spectroradiometric calibration of the temperature monitored SL 500 and SL 501 radiometers in solar radiation is estimated to be ± 14% and ± 11%, respectively (*Leszczynski et al.*, 1993).

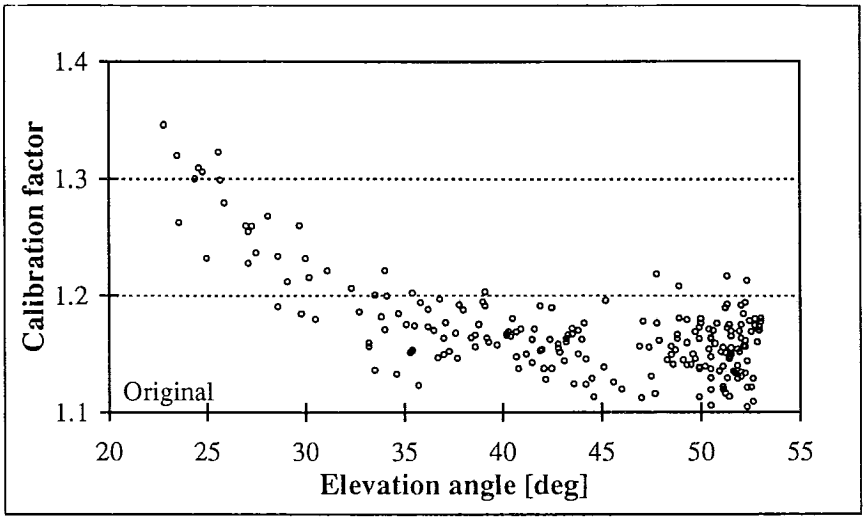

Fig. 3. The calibration factors of a radiometer SL 501 (#1452) at various solar elevation angles based on spectroradiometric calibrations.

To investigate the reason for the systematic increase of the CF:s towards lower elevation angles, the measured spectral and angular responses were used to calculate elevation angle dependent correction functions to eliminate the effects of non-ideal cosine and spectral responses. Here, the CIE-action spectrum for erythema (*McKinley* and *Diffey*, 1987) is taken as an ideal spectral response. The CF:s after applying the calculated correction functions are shown in Figure 4.

In broadband measurements, an uncertainty comparable with many spectroradiometric measurements is achievable by thorough characterisation of every meter and by spectroradiometric calibration in solar radiation at various elevation angles.

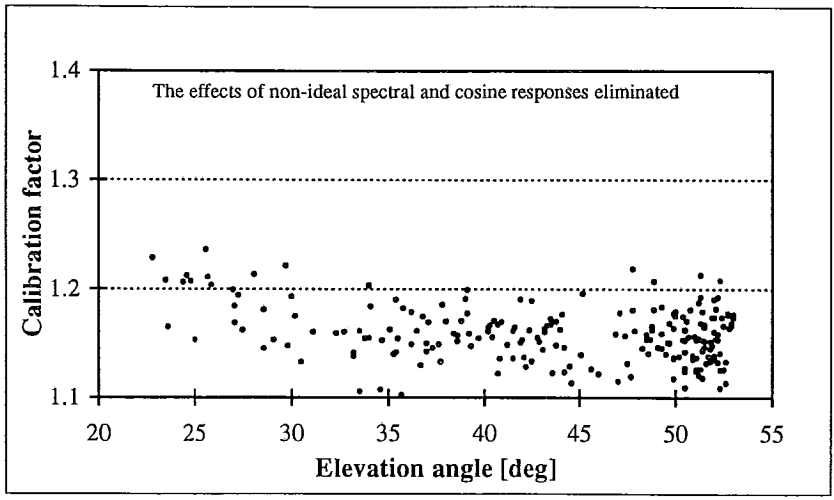

Fig. 4. Calibration factors for the SL 501 radiometer (#1452) after removing the effect caused by the non-ideal angular and spectral responses using theoretical correction functions.

2.4 Spectral UV measurements

The spectral UV measurements by using the single monochromator Brewer and external lamp calibration were started in 1990 at Sodankylä. In 1994 a double monochromator Brewer spectroradiometer was installed at Jokioinen observatory, and has been recording global UV spectral irradiance from March 1995 on. The instrument scans the wavelength range of 286.5 to 363.0 nm with 0.5 nm steps in about eight minutes. The scans are repeated about once per hour through the daylight period.

The irradiance calibration of the spectroradiometer is traceable to the UV scale of NIST (National Institute for Standards and Technology, U.S.). This calibration was checked in an intercomparison of 11 other European spectroradiometers at Ispra in May 1995 and found excellent (*Gardiner* and *Kirsch*, 1995). The wavelength calibration of the instrument was also found good. The stability of the instrument has been monitored once a week with an external UV light source. The calibration was found to be stable within ± 2.5% over the whole wavelength region.

2.5 Models of stratospheric chemistry and dynamics

The task of developing numerical modelling was undertaken in 1993 as a part of the national SILMU ozone research effort. The work has been performed in close co-operation with the atmospheric modelling group at the University of Oslo in Norway. For the goals of SILMU, and beyond, the task has been focused on the implementation of a comprehensive stratospheric chemistry parameterisation in a global, three-dimensional chemical transport model (CTM).

The general idea of a CTM is to focus on atmospheric chemistry and retrieve the data on atmospheric dynamics (transport, temperatures) and radiation (temperatures, photodissociation rates) off-line. Such decoupling is necessitated by the very three-dimensionality of the modelling, which is computationally heavy. At present, the implementation work is done with a CTM of *Prather et al.* (1990), which is formulated on the NASA/GISS middle atmosphere GCM of *Rind et al.* (1988). Meteorological output from the NASA/GISS GCM is also used as transport in the CTM. The chemistry parameterization originates from *Stordal et al.* (1985), with several additions since. The currently recognised mechanisms in the gas-phase chemistry of bromine and chlorine species have been added (*Isaksen* and *Stordal*, 1986). Heterogeneous chemistry on both PSCs and background aerosol is currently included as well (*Isaksen* and *Stordal*, 1986; *Isaksen et al.*, 1990).

The implementation has now been finished and the work is currently underway to validate the performance of the model. Data from both Sodankylä and data from satellites and ground-based networks is being applied. Preliminary results show that the model captures the global features of ozone distribution, but the quantification of this capability must await the results from more extensive comparisons with observations. Activation of chlorine is also achieved in the model lower stratosphere. The model spatial and temporal resolution is adequate to capture diurnal effects, which is illustrated with an example of the modelled nitrogen chemistry. In Fig. 5, the distribution of NO_2 at 35 km are shown for the model date of January 1, after running the model for 30 days.

In the daytime middle stratosphere, the ratio of NO and NO_2 is typically found to be close to one. At night, NO is rapidly converted to NO_2, and the abundance of NO falls as the amount of NO_2 increases. Through the night, there is a slower formation of N_2O_5 at the expense of NO_2. All these diurnal features are clearly exhibited in Fig. 5. In the morning, N_2O_5 is rapidly decomposed by photolysis, which re-establishes the daytime relationship between NO and NO_2. In Fig. 5, one can also note the zonal variation of the length of the sunlit portion of the diurnal cycle and the regions corresponding to the polar night (Northern hemisphere high latitudes) and the polar day (southern hemisphere high latitudes). In the polar night region, the conversion of NO and NO_2 into N_2O_5 has been complete. In the polar day region, the NO and NO_2 remain in their daytime balance at all local times.

In 1995 co-operation between FMI and the National Centre for Atmospheric Research (NCAR), USA in the field of modelling of stratospheric chemistry and dynamics was started. FMI is using 2- and 3-dimensional models of stratospheric chemistry and dynamics developed by the group of Dr. Guy Brasseur at NCAR. The co-operation has started by improving the photochemistry scheme during the high solar zenith angle conditions.

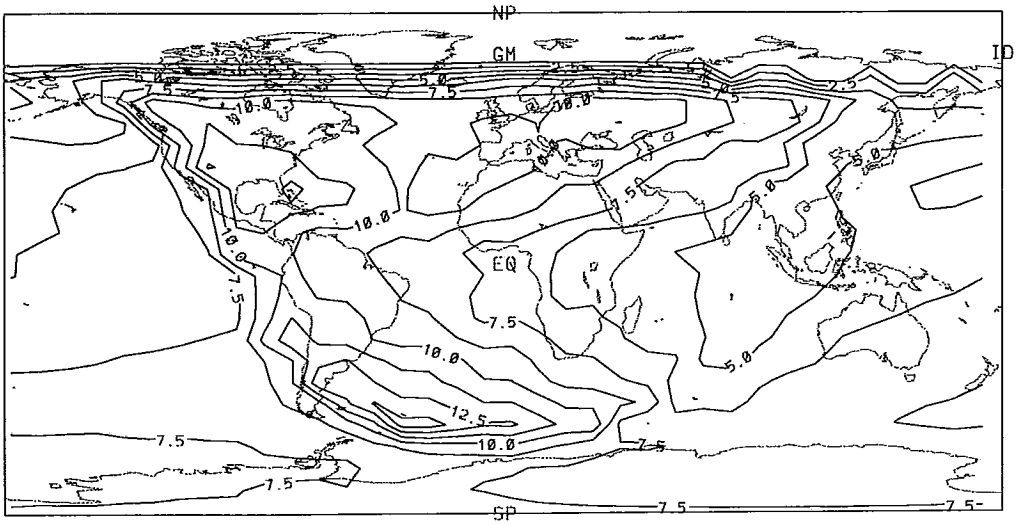

Fig. 5. Volume mixing ratio (ppbv) of NO_2 at 35 km. The plot corresponds to January 1 model date at 00 UTC.

3. *Tropospheric and lower stratospheric temperature changes*

From meteorological point of view the free atmospheric radiosounding records are especially valuable for climatic change studies, since the boundary layer meteorological records may be more subject to small-scale changes of local nature. The length of quality-controlled radiosounding records is limiting their use for climate change studies.

3.1 Radiosounding temperature trends

Taalas et al. (1995) have performed tropospheric and lower stratospheric temperature trend analysis for Jokioinen (1961-93) and for Sodankylä (1965-93), based on the radiosounding data homogenised and corrected by *Huovila* and *Tuominen* (1990). They found a warming temperature trend in the lower and middle troposphere and a cooling trend in the lower stratosphere. Largest warming occurred at 850 hPa level, i.e. 0.28 K/decade at Jokioinen, and 0.16 K/decade at Sodankylä. Largest cooling

was observed at the 70 hPa level, i.e. -0.30 K/decade and -0.24 K/decade, respectively. At Sodankylä a secondary minimum was found at 300 hPa level (0.28 K/decade).

For this study additional years of old Sodankylä radiosounding data have been corrected and digitised. The result of a linear trend analysis for 1958-94 is shown in Fig. 6 both for corrected and uncorrected data. As expected the corrected data gives smaller negative trends. Despite of that the results suggest that there might have been statistically significant (at 95 % confidence level) cooling in the upper troposphere and in the lower stratosphere between 400 and 250 hPa as well as above 100 hPa. The negative trend peaks at the 300 hPa level (-0.27 K/decade). The statistics including the additional years are good up to the 200 hPa level (~90 % of balloons reaching that level right from the beginning of the period). The statistics on the three topmost levels of 100, 70 and 50 hPa are successively poorer during five first years, but by 1964 the 90% success rate is reached even at the 50 hPa level.

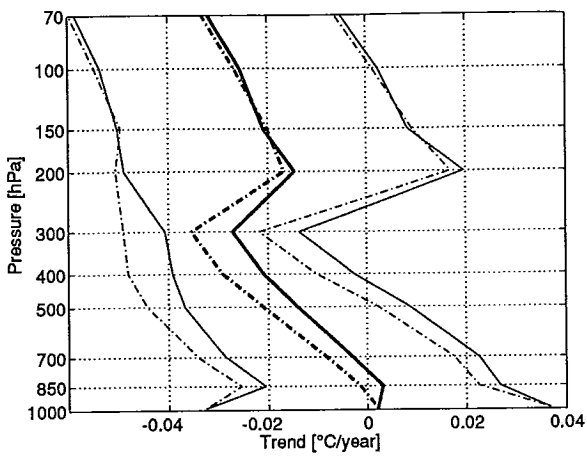

Fig. 6. Annual mean temperature trends from 1958 to 1994, calculated from 12 UTC soundings made at Sodankylä. The solid line shows the trend with and the dashed line without the lag error correction taken into account. The thinner lines show the 95 % confidence interval.

3.2 Occurrence of cold stratospheric temperatures

Since long record quality-controlled Arctic radiosounding records of lower stratospheric temperatures is available from Jokioinen and Sodankylä, the data may be used for a qualitative study of possible changes with regards to the favourable conditions for PSC formation. To make the study simple we have studied the occurrence of temperatures below 195 K at 50 hPa level at Sodankylä (Figure 7). From Fig. 7 it is obvious that the occurrence of cold temperatures in January has increased

with time with a maximum in 1995, which was also found by *Taalas* and *Kyrö* (1994). This may suggest enhancement in the formation of PSCs in the Arctic. In February the change is not as obvious. In March the cold temperatures have only been observed in 1983, 1986, 1994 and in 1995.

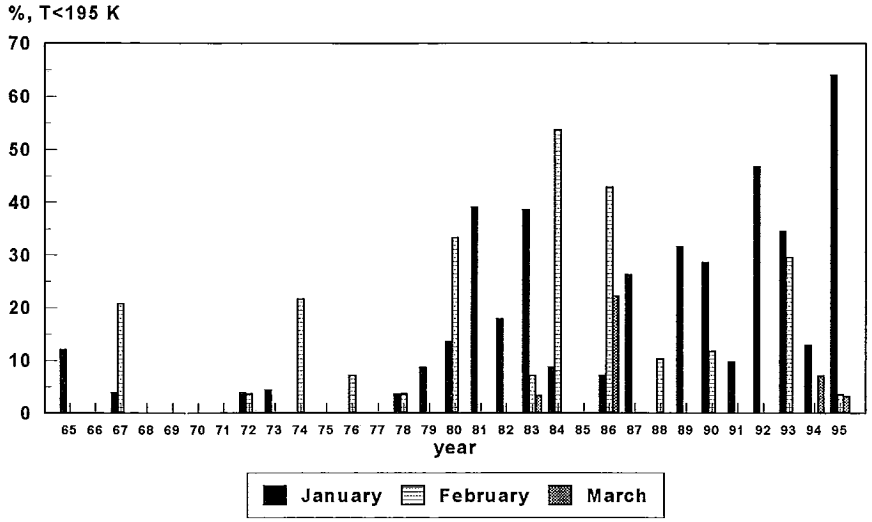

Fig. 7. Occurrence of 50 hPa level temperatures below 195 K at Sodankylä during January, February and March in 1965-95.

4. *Trends of ozone*

4.1 Total ozone

The long term total ozone data from Sodankylä are available from two sources: the TOMS satellite data set for the period 1979-1994 and local Brewer measurements from 1988 onwards. It has been shown earlier that the two data sets agree very well for the earlier Nimbus TOMS period of 1979-1991, which can also be seen from Figure 8 (*Kyrö*, 1993). For the years 1993-1994 Meteor-TOMS values have been used and the agreement is occasionally poorer than that for Nimbus-TOMS. After November 1994 there has been no TOMS data available because of the break down of the instrument.

The annual mean trends are estimated for the three seasons: winter, summer and autumn. The definition is made according to the polar stratospheric seasons. April is left out because it is typically the transition period from westerly winter circulation to easterly summer circulation (*WMO*, 1991). The trends in Figure 8 refer to those calculated from TOMS data set which is longer than the Brewer record of Sodankylä. Corresponding Brewer trends for 1988-94 are significantly larger, i.e. -25.1 ± 7.3)%/decade for winter, -6.0 ± 5.1%/decade for summer, and 10.0 ± 3.4%/decade for

autumn by using one sigma errors. The winter trend is large partly because of the exceptionally high ozone values in the beginning of the Brewer series in 1989. Starting from 1990 yields the Brewer trend of -16 % per decade, which is still double the TOMS trend for the whole period 1979-94. The acceleration of the downward trend towards the end of the period is obvious from Figure 8. *Taalas* (1996) has studied the reason for the year-to-year variations of total ozone seen in Figure 8, and found out that dynamical factors explain most of these.

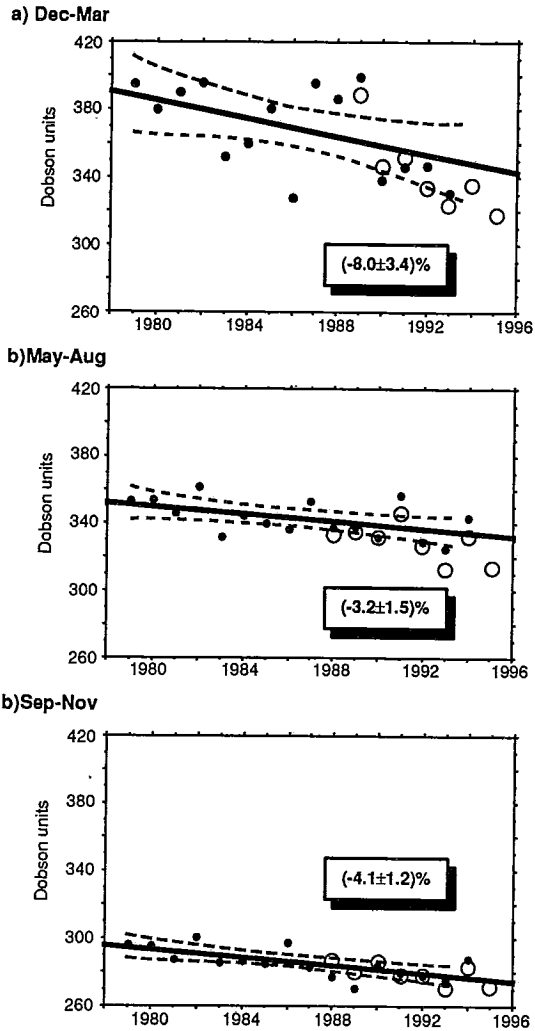

Fig. 8. The trends of total ozone at Sodankylä as calculated from the TOMS satellite instruments for the 15 year period 1979-1994. Unit %/decade. TOMS data are shown as full circles. For comparison, the ground based Brewer observations for the period 1988-1995 are plotted as open circles. The 95% confidence interval is indicated by dashed lines around the linear trend line.

4.2 Vertical distribution of tropospheric ozone

The results from nearly 500 ozone soundings made at Sodankylä after the start of the regular sounding programme in 1988 show that tropospheric ozone undergoes a regular annual variation at Sodankylä. At the surface, ozone levels peak in April-May, whereas in the free troposphere, ozone levels peak in June. The high summer values in the free troposphere are indicative of transport of anthropogenic pollution from Central Europe (*Taalas et al.*, 1993; *Mikkelsen et al.*, 1994; *Rummukainen et al.*, 1996).

There are but a few available studies on tropospheric ozone trends. In Central Europe, as well as in Japan, a positive trend has been found for ozone in the free troposphere between late 1960's and 1980's (*Logan*, 1994; *Akimoto*, 1994). In Canada, there seems to have been a slightly negative ozone trend in the free troposphere (*Oltmans*, 1993; *Tarasick et al.*, 1995). These few existing studies do not cover the European Arctic region. Even the longest data series in the region, that of Sodankylä, is still rather short for trend assessment. The preliminary analysis of the data features decrease of ozone with time in the troposphere. In this analysis, ozone trends are calculated in five layers from the surface to the lower stratosphere. For the lower and middle troposphere, the trends are calculated in three layers: surface-800 hPa, 800-600 hPa and 600-400 hPa. For the upper troposphere, the trend is calculated in a 100 hPa thick layer located just under the tropopause. In the lower stratosphere, the trend is calculated for a layer of approximately comparable thickness, located just above the tropopause. The tropopause is defined as a Potential Vorticity level of 1.6 10^{-6} $m^2kg^{-1}s^{-1}$, *WMO* (1985). The yearly results are summarised in Table 3 below. The year-round data have been deseasonalised as in *Logan* (1994).

The tropospheric trends are negative with a magnitude of -2 %/year. Trends in the lower stratosphere, just above the tropopause, are not significant. The deseasonalizing procedure does not have a large effect upon the annually averaged trends, as the scatter in the data is of a similar magnitude as the seasonal variation. The seasonal trends have also been analysed from these data by *Isaksen et al.* (1995). The only significant seasonal trend was in the summer (June-August), for which the trends were -5.0 ± 1.6 %/y, -4.0 ±1.1 %/y and, -4.8 ± 1.1 %/y in the three lowest layers, and -4.2 ± 1.4 %/y (one standard error) in the layer just below the tropopause. In the layer below tropopause no significant trend was found even in summer. For the other seasons, autumn (SON), winter (DJF) and spring (MAM) all the trends were not significant.

Taalas et al. (1993, 1996) have studied the reasons for tropospheric ozone deviations in the Arctic and at Antarctica. They have shown a link between stratospheric and upper tropospheric ozone variations at monthly mean level. The pronounced downward trend in stratospheric ozone at the high latitudes may also have affected the tropospheric ozone trends due to changes in the photochemical activity and in the flux of ozone from the stratosphere to the troposphere.

Table 3. Trends of the ozone mixing ratio [ppbv] in 1989-1994, averaged through tropospheric layers of surface-800 hPa, 800-600 hPa, 600-400 hPa, through a 100 hPa layer just below the tropopause and through a comparable layer just above the tropopause. The intercept is for Jan 1, 1989, and the trend is the slope of the regression line divided by the mean value over the hole period. Trends are considered significant if they exceed two standard errors (Isaksen, et al. 1995).

Level	Intercept (ppbv)	Std. error (ppbv) %/year	Trend %/year	One standard error %/year	Significance
Sfc-800 hPa	40.3	1.0	-2.2	0.5	yes
800-600 hPa	52.6	1.0	-2.0	0.4	yes
600-400 hPa	64.3	1.2	-2.3	0.4	yes
Below tropopause	73.0	1.8	-2.3	0.6	yes
Above tropopause	203.2	9.2	-0.5	0.9	no

5. *Arctic ozone anomalies 1989-95*

At Antarctica largest ozone anomalies are observed inside the polar vortex with clear indications of heterogeneous chlorine and bromine chemistry as the dominant factor behind ozone deviations. In the Arctic the picture is less clear due to more intense dynamical activity, which leads to warmer and less stable polar vortex. Exchange of airmass between the vortex core and the airmasses outside of the vortex is frequent. On the other hand wave activity may lead to existence of local ozone anomalies due to vertical redistribution of stratospheric ozone.

Isentropic time series analysis has been widely used for getting indirect information of possible chemically induced ozone loss in the Arctic (*Kyrö et al.*, 1992; *Braathen et al.*, 1994 and *Knudsen et al.*, 1994).

5.1 Variations of stratospheric ozone at isentropic levels in 1992 and 1995

During the two winters of 1991/92 and 1994/95, extensive European ozone campaigns took place in the Arctic. As a part of these campaigns, numerous ozone sondes were launched inside the polar vortex. The amount of ozonesounding data makes it possible to perform isentropic analysis for these two winters. In addition, the temperature evolution during these two winters were very different (*Pawson et al.*, 1995). In 1991/92, the winter was first cold, but after the strong stratospheric warming event in January, the rest of the winter remained quite warm. This probably prevented much of the potential ozone loss from occurring towards the spring. In 1994/95, extreme coldness prevailed from December until early February, and there were also a few cold spells later in the winter. Isentropic analysis of ozone at 475 K potential temperature surface inside the polar vortex has been applied on the Finnish data at Sodankylä in 1991/92 and 1994/95 and at Jokioinen in 1994/95. The results are shown in Figure 9.

A linear model was applied to the daily ozone data at the 475 K isentropic level. In 1992 the ozone change above Sodankylä was -0.07 ± 0.07 %/day for the three month period of January-March. In 1995, the corresponding change was -0.31 ± 0.05. Clearly, the interannual variability in the isentropic ozone loss rates is quite large. Visual inspection suggests that the variability is large within the individual winters as well, which makes trends derived for shorter periods than a whole winter sensitive for the choice of the averaging period. It is not attempted to derive the variability of the 475 K ozone trends within either of these two winters from the Finnish data alone. However, such work has been done with all of the EASOE ozone sounding data in 1991/*92 (von der Gathen et al.*, 1995) and with all of the SESAME ozone sounding data in 1994/95 (*Rex et al.*, 1995). The rate of diabatic descent has been taken into account in these two studies. In 1991/92, ozone loss rates at 475 K were large in the end of January, and they reached -1.7 ± 0.3 %/day for a brief period. Preliminary results for the loss rate at 475 K in 1994/95 indicate a similar maximum loss rate for January and also for mid-March. Even though the maximum loss rates were comparable in 1992 and 1995, the total ozone loss was much larger in 1995 than in 1992.

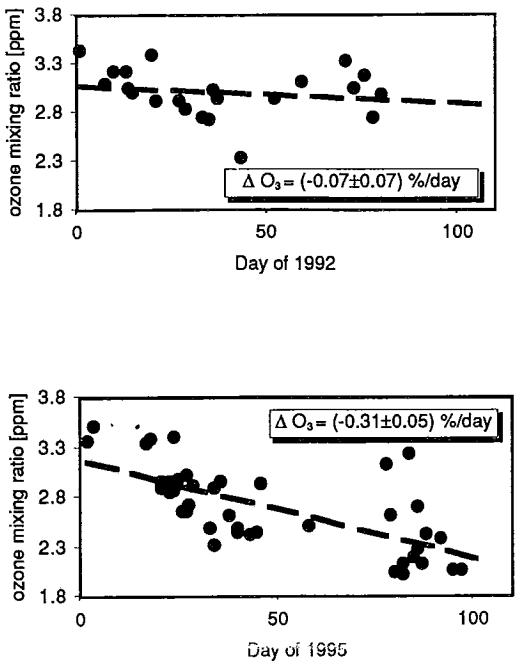

Fig. 9. Development of ozone mixing ratios at 475 K inside the Arctic polar vortex in January-March of 1992 and 1995 at Sodankylä. Linear trend ± one standard error are shown.

The estimates from the Finnish data for the chemical ozone loss in the winters of 1992 and 1995 above should be taken as the lower limit for the chemical ozone loss in side the vortex. The positive contribution to ozone at 475 K, through diabatic descent, has not been taken into account. This contribution is examined more closely for the latter winter in the section below.

5.2 Possible indications of chemical ozone loss inside the polar vortex in January-March 1995

In this section, the chain of the events leading to large scale ozone depletion inside the Arctic polar vortex in January-March 1995 is illustrated with experimental results on PSC occurrence, observation on elevated chlorine levels and the changes in lower stratospheric ozone. Due to the extreme coldness of the Arctic lower stratosphere in the winter of 1994/95, there was a large potential for the formation of PSCs. At Sodankylä, PSCs were seen in every backscatter sounding made between December 22, 1994 and January 19, 1995. The concurrent multi-wavelength, two-polarization aerosol lidar experiment at Sodankylä reported PSC-observations until January 26. The findings of the lidar experiment support the present views that depending on the thermal history of the air parcels, PSC particles can be of different composition, phase and shape. Following the classification introduced recently by *Tabazadeh et al.* (1994), PSCs consisting of solid SAT (Sulphuric Acid Trihydrate), STS-droplets (Supercooled Ternary Solutions), NAT-particles (Nitric Acid Trihydrate) or water ice particles were detected in December-January 1994/95 (*Stein* and *Adriani*, 1995; *Stein et al.*, 1995). As an example of the PSC observations at Sodankylä, the backscatter sounding made in January 19 is presented in Figure 10. The temperatures were just at the threshold of water ice formation in the narrow vertical range of 470-500 K (21-22 km). The minimum temperature of -87.6 °C occurred at the 500 K isentropic level, close to the very high backscatter ratio of 50, measured at the 940 nm channel.

The frequent PSC occurrences during the early part of the winter led to an efficient activation of chlorine, much in the same way that has been seen to occur prior to the formation of the Antarctic ozone hole. For example, on February 3, highly enhanced ClO was measured inside polar vortex near Sodankylä, which is shown in Figure 11. The layer of high ClO, up to 1.3 ppbv, extended vertically from 450 K to 550 K, which should be compared to the background levels of less than 0.1 ppbv (*WMO*, 1994).

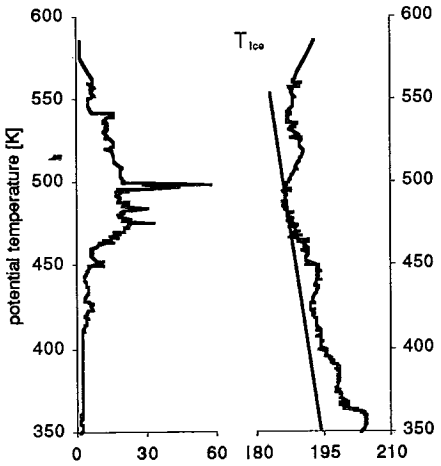

Fig. 10. Vertical distributions of aerosol backscatter (left) and temperature (right) in January 19, 1995 at Sodankylä. Typical threshold temperatures for the formation of water ice droplets at each altitude are also shown as a full nearly straight line in the right hand picture.

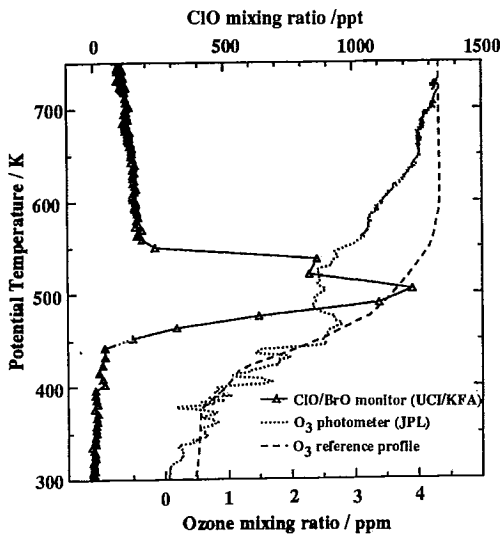

Fig. 11. ClO-profile from the KFA Julich balloon experiment at Kiruna (68 °N, 21 °E), February 3, 1995. The maximum error is estimated as 30%. Simultaneously measured ozone profile is depicted with the dotted line. In the absence of chemical depletion, ozone would be expected to exhibit the distribution given with the stippled line (D. Toohey, private communication).

The nature of the ozone loss in 1995 can actually be quantified with the ozone sounding data at Sodankylä. This is shown in Figure 12, where the soundings of January 28 and March 21 are compared. They were both made deep inside the polar vortex with potential vorticity values of 52 and $55*10^{-6}$ $m^2kg^{-1}s^{-1}$, respectively at 475 K isentropic level. Between January 28 and March 21, ozone was reduced in a thick region throughout the lower stratosphere inside the polar vortex. The loss is visible in the 360-500 K range and the maximum loss reached 55 % at 450 K (about 18 km). At 475 K, the loss was 25 % during this period. This would correspond to a mean trend of -0.48 %/day over the period, which is higher than the trend of -0.31 %/day, which was analysed for the whole winter. This is an indication of variability of ozone loss within the winter which depend on the development of the chemical state of the vortex air and solar radiation.

Already in January/beginning of February, there has evidently been ozone loss at 450 K and above. This can also be seen in figures 10 and 11. The visible loss by the end of March is largest at around 450 K and below. The change in the profile shape, and the change in the apparent region of maximum loss in Fig. 12 is partially due to diabatic descent inside the vortex. In the lower stratosphere, some of the chemical ozone loss must have been masked by diabatic descent through the vertical gradient in the ozone mixing ratio profile. The observed and analysed mid-winter subsidence rates are of the order of a few tenths of a Kelvin per day at the 475 K level. In mid-winter, they have been found to reach up to 0.7 K/day (e.g. recent work by *Rosenfield et al.*, 1994; *Strahan et al.*, 1994). As a typical vertical gradient of ozone at 475 K is of the order of 0.02 ppmv/K, a subsidence rate of 0.7 K/day would amount to a positive trend in ozone at 475 K of the order of 0.5 %/day. This mid-winter figure is certainly too high, if it were applied for the whole period from January to March, so it should be taken as an upper limit for this period. The upper limit of the chemical ozone loss at 475 K is then the sum of the observed negative trend at 475 K and the estimated trend due to diabatic descent, which results in the chemical ozone loss 1.0 %/day between late January and late March in 1995. This is more than half of the maximum loss rates seen for the winter (*Rex et al.*, 1995).

5.3 The occurrence of total ozone anomalies versus 50 hPa temperature

A high frequency of stratospheric ozone anomalies have been observed in the Arctic during recent years. The location of the polar vortex and the stratospheric temperatures is of interest to give hints of the possible reason for the anomalies.

In this work the 1935-69 total ozone means of Tromsö, as recalculated by *Bojkov* (1988) have been used as a reference. Anomalies of 10 % and greater from those at Sodankylä have been picked out for further analysis. The anomalies have been classified according to the 50 hPa temperature observed at Sodankylä. The frequency of total ozone anomalies according to 50 hPa temperature is shown in Figure 13. It is obvious that most of the anomalies observed in the European Arctic during recent years

have been connected to "warm" 50 hPa temperatures. This may mean low probability for the occurrence of PSCs in the airmass, which suggests a considerable difference as compared with the Antarctic ozone loss morphology.

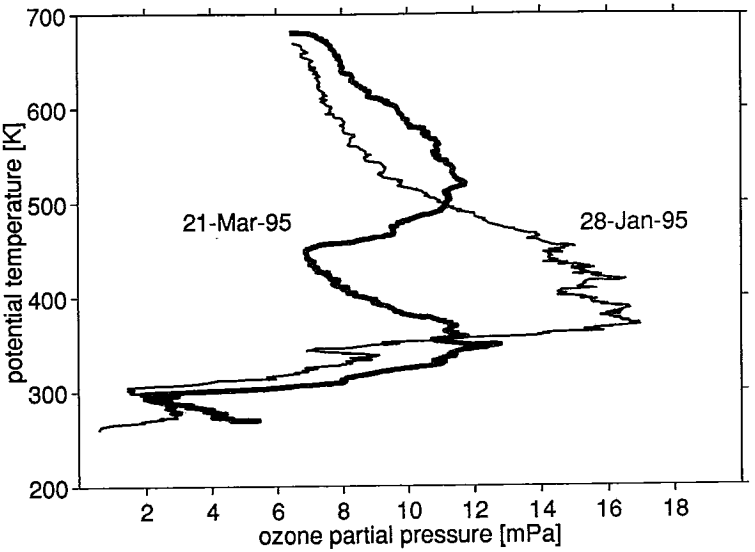

Fig. 12. Ozone soundings in January 28 (solid line) and March 21, 1995 (dotted line).

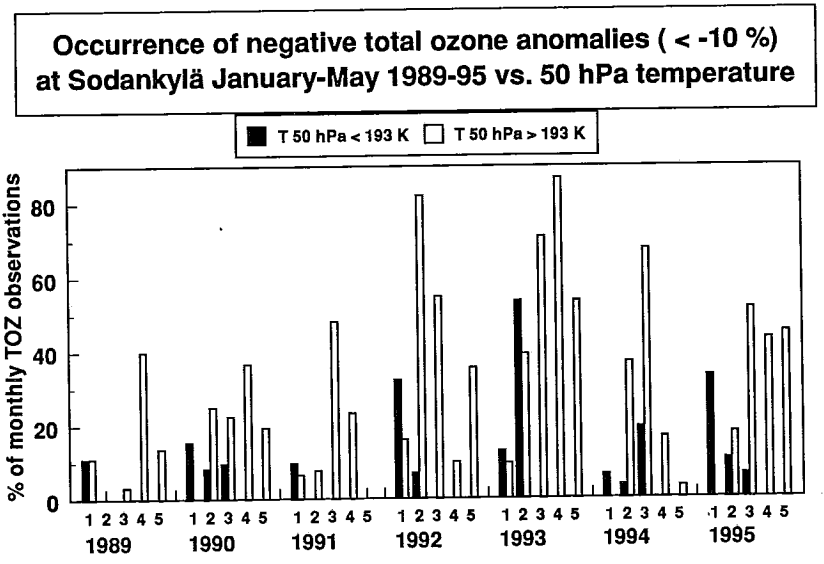

Fig. 13. Occurrence of negative total ozone anomalies (< -10 %) at Sodankylä January-May 1989-95 versus 50 hPa temperature.

6. *Climatology of solar UV radiation in Finland*

6.1 The effect of total ozone on UV radiation

The radiative transfer of solar UV radiation through the atmosphere is theoretically quite well known. Therefore the absorption of solar UV-B radiation by the atmosphere can be modelled. In this section the UVDOSE (*Dahlback* and *Stamnes*, 1991) model is used for calculating the clear-sky UV-B irradiances. Erythemal weighting function (CIE) and a constant surface albedo of 20 % have been applied. The daily total ozone record made at Sodankylä 1987-95 has been used. Data has been interpolated for the days with no total ozone measurements. The long-term total ozone values used as references are the 1935-69 means at Tromsö. Daily clear-sky UV doses have been calculated for Sodankylä by using the actual measurements and the long-term means of total ozone. The usefulness of the modelling treatment is based on the fact that it allows estimation of UV irradiances from a longer period in Finland than just the UV observations.

The monthly doses for 1987-95 and their deviations from the modelled long-term means are shown in Figure 14. From the figure is seen that the springtime clear-sky UV doses have exceeded the long-term means almost every year with largest deviations in 1993 (relative maximum +24.1 % in April). Summer deviations have been observed during 1992-95 with a maximum of +13.4 % in June 1995. The deviations are relatively small as compared to those calculated for the same latitudes at the Southern Hemisphere (*Taalas et al.*, 1996).

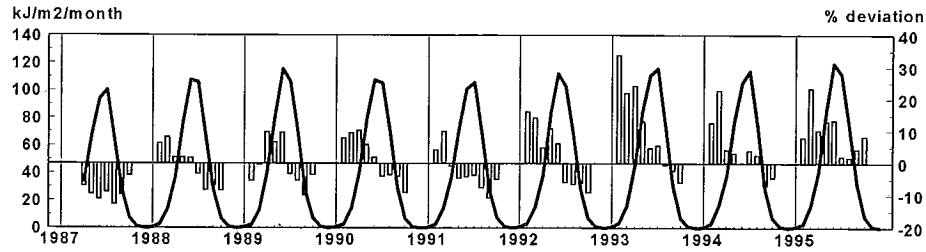

Fig. 14. Calculated CIE-weighted clear-sky UV-B doses (line) and relative deviations from 1935-69 means at Sodankylä (columns, November-January excluded), Finland April 1987-December 1995 (see text for details).

6.2 Observed erythemal UV irradiances at Jokioinen

The broadband UV data were recorded as 15-minute averages. These were corrected for the temperature dependence of the detector according to *Koskela et al.* (1994). The calibration of the detectors is traceable to NIST (National Institute of Science and Technology, U.S.) via the OL-742 spectroradiometer of STUK and its

1000W FEL-type lamp. The calibration coefficient was adjusted to take into account the difference of the actual CIE erythemal action spectrum and the measured spectral sensitivity of the particular detector. Although the influence of the spectral difference depends on the total ozone column and solar zenith angle (SZA), a constant calibration coefficient valid for normal ozone and small SZA was used. Therefore a small underestimation of the daily UV sums during the winter season can be expected. No cosine correction, so far, was applied to the broadband data.

In Figure 14 the potential "ozone forcing" on UV-B radiation was shown. In the real atmosphere especially cloudiness is affecting the variation of UV irradiances. In general the modelled annual clear-sky UV-B doses have varied between 434 kJ/m^2 (1991) and 490 kJ/m^2 (1995), which is of the order of 40 % higher than the observed annual doses in 1993-95.

Qualitatively most of the features of Figures 14 and 15 for 1993-95 agree fairly well, i.e. relative deviations caused by ozone loss are also seen in Fig. 14 while performing comparisons within certain months (March 1994, April & May 1993 and June 1995). On the other hand the highest observed monthly dose in July 1994 is mainly related to unusually cloud-free high-pressure system observed in Finland.

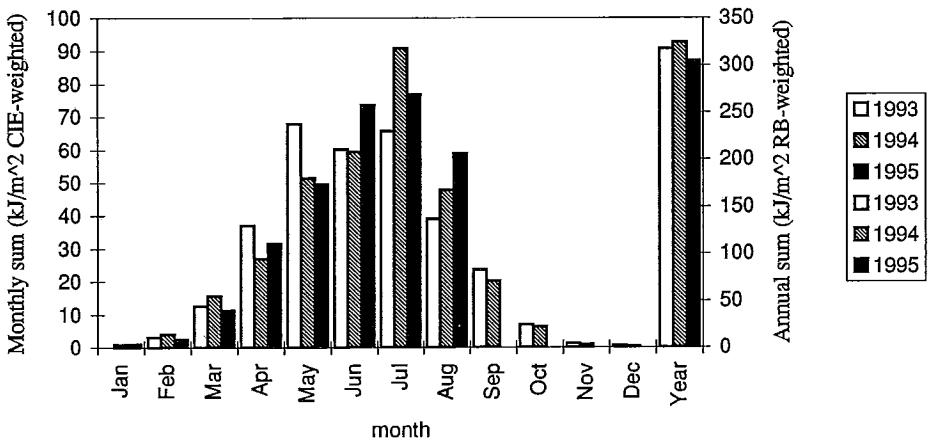

Fig. 15. Observed erythemal UV irradiances 1993-95 at Jokioinen. In 1995 data for September-December is not accounted, which makes the annual dose about 10 % too low.

6.3 Spectral distribution of UV radiation

It is also important to study the UV irradiances observed with the spectroradiometers due to higher accuracy. On the other hand the spectral observations using Brewer Mk. III with extended wavelength band are important for studying various biological processes affected by solar UV radiation.

Biologically effective daily doses were calculated from the spectral measurements by using the following weight functions or action spectra (Fig. 16), that were normalised at 300 nm, if not stated otherwise:

(1) CIE Erythema, normalised at 298 nm

(2) SCUP-m, normalised at 293 nm

(3) UV-B (non-weighted)

(4) General plant response

(5) Photosynthesis inhibition

(6) DNA

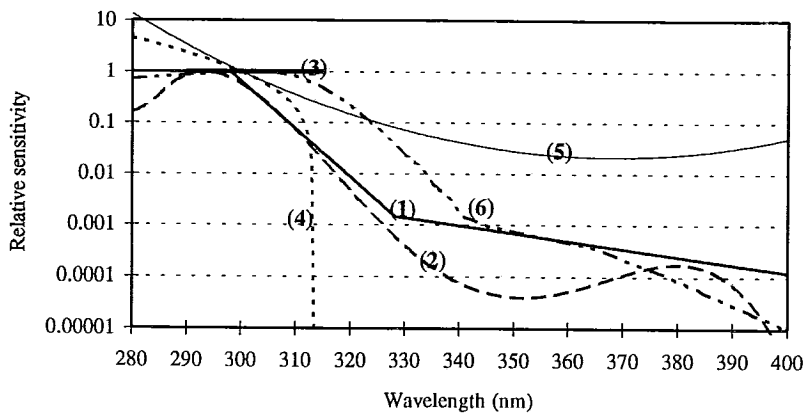

Fig. 16. Action spectra used in calculating the biologically effective doses. Labels (1) to (6) are explained in the text.

The results are shown in Fig. 17 and can be readily used as an order-of-magnitude estimate of the UV exposure at an inland location on the 60ºN latitude.

Many of the biological weighting functions (action spectra) extend up to 400 nm in the wavelength scale, while the Brewer instrument only measures up to 363 nm. A method was developed to correct for this missing part of the spectrum between 363 and 400 nm. The method is based on the fact that the irradiance in these wavelength depends only little on ozone column abundance, and the shape of the spectrum is very

repeatable although the absolute value varies with solar zenith angle and cloud thickness. Therefore, the irradiance measured at the wavelength of 361 nm, where the spectrum is relatively flat and small errors in wavelength calibration will not become significant, could be used to adjust a so-called relative spectrum (RS) to its correct level in the irradiance scale. The relative spectrum, on its side, was obtained by the analysis of nearly 50 quality controlled full-length spectra measured at Ispra in May 1995 by two Bentham instruments. According to this limited data set the RS-method seems to able to reproduce the true spectra between 363 and 400 nm with an accuracy of ±15% when the solar zenith angle ranged between 25 and 73 degrees. The error e.g. in the erythemally weighted dose rates was below 0.5% and in the daily dose below 0.05%.

Daily doses were calculated by integrating the area under measured dose rates with a trapezoid-method. The scans were required to start near the sunrise, end near the sunset, take place at an interval of three hours or less, and have a maximum step of 20 degrees in the solar zenith angle of two successive measurements.

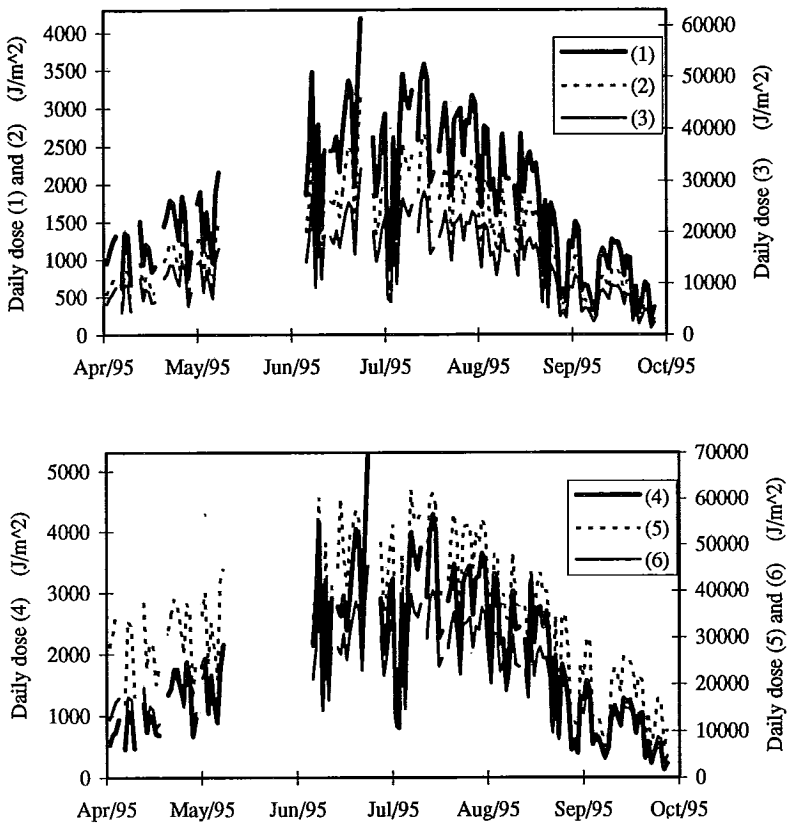

Fig. 17. Daily UV doses weighted by action spectra (1) to (6) during 1 April to 30 September 1995 at Jokioinen Observatory (60º49'N, 23º30'E). The action spectra are explained in the text.

At the same location as the Brewer spectroradiometer, erythemal irradiance was monitored at high time resolution with a broadband Robertson-Berger UV radiometer. The daily erythemal doses measured by these two independent methods correlate well (R2=0.98), but the broadband meter shows as an average through the season 7.5% lower values. This difference is within the estimated accuracy of the instruments, but can also be explained partly by differences in cosine response and the difference of the spectral responsivity of the meter from true erythemal action spectrum.

7. *On the future development of stratospheric ozone content in the Arctic*

The stratospheric ozone scenarios presented some years ago have certain limitations, and are therefore not adequate for UV-B scenario calculations. Knowledge of the behaviour of stratospheric ozone has increased considerably during recent years. The discovery of heterogeneous reactions behind the Antarctic ozone loss and the potential effect of atmospheric CO_2 content on the polar vortices have been the most important factors that have weakened the validity of former ozone scenarios. *Austin et al.* (1992) and *Austin* and *Butchart* (1994) have demonstrated that a doubling of atmospheric CO_2 content may lead to a more stable polar vortex in the Arctic. Although additional model runs by different models are needed to verify those of *Austin et al.* (1992), we have used the "Arctic ozone hole" scenario to get an idea of possible future UV-B changes in the Arctic. In this ozone scenario a doubled CO_2 content and its consequences on global atmospheric dynamics may lead during certain years to a prolonged existence of the Arctic polar vortex, even until early May.

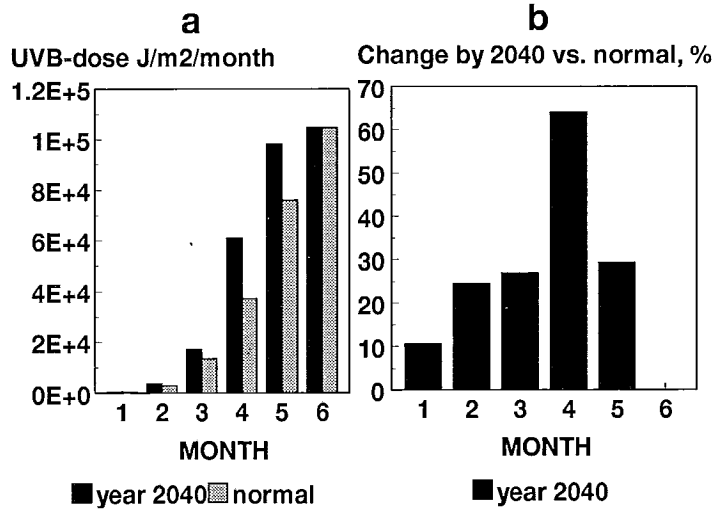

Fig. 18 a and b (*Taalas et al.*, 1995). A scenario for erythemal UV-B radiation for 2040. Absolute (a) and relative (b) changes in a CO_2-doubled atmosphere, "worst case"-scenario for ozone. See text for details.

We have used the latitude minimum of total ozone from *Austin et al.* (1992) to construct a worst-case UV-B scenario for the 67 °N latitude. The absolute and relative UV-B dose changes may be seen in Figures 9a and 9b. As can be seen, the biggest relative change of 64.1% occurs in April. The annual dose increases in the scenario by 11.2%, as compared with the "normal".

8. *Personal exposure to solar UV*

The major consequence of the ozone depletion is the increased exposure of human populations and ecosystems to solar UV radiation up to 320 nm. Two action spectra are most relevant for the human health assessments. The action spectrum for the human erythema (Fig. 16, curve 1) has been defined by CIE on the basis of experimental data with human beings (*McKinley* and *Diffey*, 1987), while the SCUP-h action spectrum for the non-melanoma skin cancer has been derived from experimental data for mice (Fig. 16, curve 2) corrected by taking into account the thickness of human epidermis (*de Gruijl* and *van der Leun*, 1994).

The CIE action spectrum has been used extensively since 1987 for theoretical and experimental exposure assessments. Calculations performed in this study with the radiation transfer model of *Green et al.* (1980) show that the ratio of the annual SCUP-h dose to the annual CIE dose varies only from 2.01 at 70 ºN latitude to 2.17 at the equator (average 2.13). Hence, the SCUP-h values can be derived relatively accurately with a simple scaling from the CIE values.

The actual exposure received by different individuals is only a small fraction of the maximal UV doses available on a horizontal plane in the living environment. *Schothorst et al.* (1987) estimated that the outdoor workers receive in average 5.4% and the indoor workers 2.7% from the maximal available (horizontal) annual doses. The individual exposure and its distribution over the body depends largely on the local environmental factors (e.g. reflection from the snow), clothing, personal protection (sunscreens and protective glasses), the time spent outdoors and the form of outdoor activities.

The face is the part of the human body, which may receive relatively high cumulative UV doses. In the Arctic and Subarctic regions a significant amount of the facial UV dose may be due to the reflection of UV from the snow (*Jokela et al.*, 1993; *Jokela et al.*, 1995). For the fresh snow the reflection (albedo) may be as high as 94 % (*Blumthaler* and *Ambach*, 1988). In Northern Europe it is possible that snow increases significantly even the annual UV doses of population. The terrain may be covered by snow in late spring months, when the UV levels are sufficiently high to cause biological effects. Ozone loss may, on the other hand, intensify this effect considerably during spring in the Arctic.

It is obvious that the exposure on vertical surfaces describes better the facial exposure than the exposure on the horizontal surfaces. In Figure 14 the clear-sky erythemal UV doses received on horizontal surfaces at Sodankylä was shown. As was seen in Fig. 15, under real atmospheric conditions cloudiness may play a significant role affecting the observed UV doses. It is interesting to study theoretically the effect of snowcover on vertical and on horizontal surfaces. Calculated clear-sky UV doses under various circumstances are shown in Figure 19. Daily clear sky doses as a function of solar zenith angle have been calculated for skiing resort Saariselkä in Northern Finland (68.4 °N, 27.5 °E) by using the Green's model (*Green et al.*, 1980; *Jokela et al.*, 1993). A simple algorithm (*Bird* and *Riordan*, 1986) was used to convert the horizontal irradiance to the vertical irradiance averaged over the full 360 degree compass angle. The highest and lowest curves were computed by using the long term mean of the total ozone values measured at Tromsö (69.7 °N, 18.9 °E) (*Taalas*, 1993). The irregularly plotted line shows the results computed by using the actual total ozone measured at Sodankylä. For the winter, albedo of 0.8 was adopted, which decreased linearly to the summer value of 0.04 during a period of 25 days before the end of the snow season (16 May). In autumn the change was assumed to be abrupt (24 Oct.). Note that the calculated curves are realistic only for clear skies with a fresh snow. The area of the treeless terrain must be several square kilometres.

The snow reflection may increase the springtime UV exposure to face considerably at Saariselkä (see Fig. 19). In April the calculated clear-sky exposure is equal to the exposure in midsummer. The calculated snow effect is much smaller on horizontal UV doses. In Southern Finland the effect of surface albedo on both horizontal and vertical exposure may be estimated to be smaller due to typically earlier timing of the melting of the snow, before UV increases to significant levels; the terrain, moreover, is covered by trees and buildings, which effectively reduce reflections. The situation may be different at frozen lake conditions. A comparison of computed clear sky annual doses indicates that the normal horizontal CIE dose is about 29% higher in Helsinki than at Saariselkä, while the difference is only 12% for the vertical doses. Hence, the snow reflection may smoothen out geographical differences in the UV exposure.

Snow may have more striking effect on ocular doses than on facial doses, because the viewing angle of the eye is limited, and the eyes are normally directed towards the horizon and ground (*Sliney*, 1986; *Sliney* 1994). In an environment with low albedo the viewing angle is limited by the anatomical structure of eye, and the Fresnel reflection from the surface of cornea reduces the exposure to the UV rays coming in a large angle of incidence from the sun and high sky. At snow-covered areas the ocular exposure is determined by the UV rays reflected from the ground. It may be estimated that at open snow-covered areas the ratio of the corneal irradiance to the vertical irradiance varies from 0.7 to 0.9 (*Jokela et al.*, 1993).

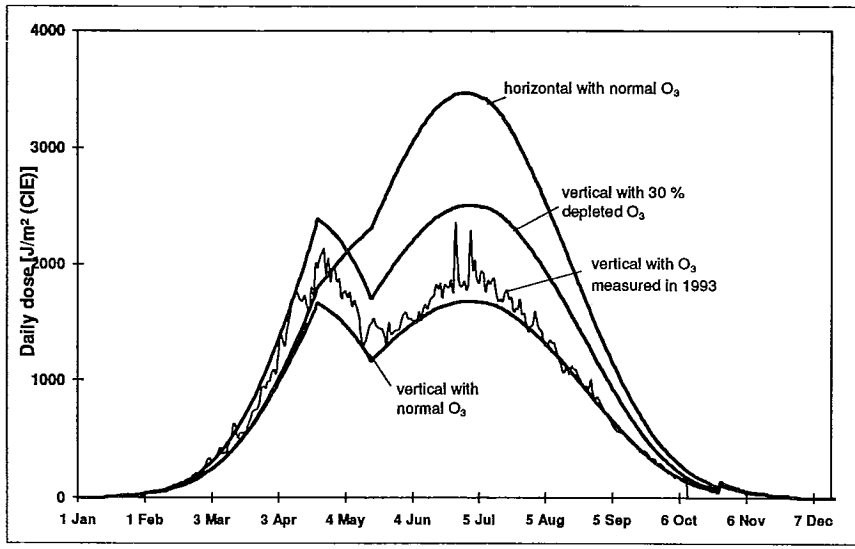

Fig. 19. Annual cycle of calculated clear-sky UV doses to a vertical and horizontal surface for normal and depleted total ozone. The irregular line shows the results obtained by using measured values for the total ozone. The smooth lines were calculated with the mean (climatological) total ozone and the mean ozone reduced by 30%.

9. *Potential health impacts of increasing UV*

The most adverse health effects of UV radiation are increased incidence of skin cancer, immune-suppression, activation of viruses in the skin, cataracts, and degenerative changes of the cornea (*Longstreth et al.*, 1995). The malignant skin melanoma is probably the most serious health effect caused by the increasing solar UV in the countries populated by fair skinned people. In Finland, where the number of population is about 5 million, melanoma causes about 100 deaths every year, while the mortality rate for the non-melanoma skin cancers is significantly lower, about 25 deaths per year. The fatalities are mainly due to the squamous cell carcinoma (SCC). The incidence of the third type of skin cancers, the basal cell carcinoma (BCC), is very high (3590 in Finland in 1986), but it is fatal only in very rare cases. In many developing countries, the possible increase of cataracts may be a significant health problem in the future, since the cataract is one of the main causes of the blindness in the conditions where the resources for lens surgery are limited. Unfortunately, quantitative risk analysis is at the moment possible only for non-melanoma skin cancers.

The increase of UV caused by the decreasing global ozone can be computed by using published depletion trends combined with radiative transfer model. The assessment of the increased incidence of skin carcinomas can be based on the calculated

clear-sky UV doses by using available epidemiological model for the relationship between the carcinomas and annual UV doses. In this study the carcinoma increase estimates of *Madronich* and *de Gruijl* (1994) are updated on the basis of the recent ozone depletion estimates presented by the World Meteorological Organization (*WMO*, 1994). Special attention is paid on the theoretical absolute increases of SCC's as a function of latitude.

Since ozone depletion and UV irradiance vary as a function of latitude and the day of the year, it is convenient to define the effective ozone depletion

$$p_{eff} = 1/D_a(\theta)\ \Sigma_i\ (D_i(\theta)\ p_i(\theta)) \qquad (1)$$

where p_{eff} is the average effective annual ozone depletion (%), D_a is the annual UV dose, p_i is the average depletion during season i and D_i is the corresponding UV dose, which all vary as a function of latitude.

The seasonally averaged depletions were computed by multiplying by 22 (years) the seasonal averaged trends (%/year) given by *WMO* (1994) for all seasons. It was assumed that before 1978 no depletion occurred, from 1978 to 2000 ozone depletes linearly. It is also assumed that after year 2000 it remains at the constant depleted level for several decades. This assumption has limitations especially in the Northern Hemisphere, where climatic factors may have an impact on the future development of ozone (see Ch. 7). The seasonally averaged trends were obtained from the average of the satellite (SBUV) and ground based (Dobson) trend data based on the measurements from 1979 to 1994 (*WMO*, 1994). For the 70th latitude the TOMS satellite data was used, because no data was available for the 70th latitude in the WMO report. The choice of the depletion period from 1978 to 2000 is not arbitrary, since before 1978 the measured ozone depletion was small and the preliminary model calculations indicate that the loss rate might become slower within the next few decades.

When the depletion is less than 20 %, the ratio of the increased annual dose to the normal (pre 1978) dose follows very accurately the exponential law given by

$$D_a(\theta,p_{eff})/D_a(\theta,0) = (1 - p_{eff}/100))^{-RAF} \qquad (2)$$

where the exponent RAF is so called radiation amplification factor. For CIE weighted annual UV doses, RAF varies from 1 at the 70 ºN latitude to 1.2 at the equator. Similarly, the animal experiments and epidemiological data indicate that the relative incidence of the carcinomas follow the exponential relationship

$$I\ (\theta,p_{eff})/I(\theta,0) = (D_a(\theta,p_{eff})/\ D_a(\theta,0))^{BAF} \qquad (3)$$

where I is the age adjusted annual incidence and BAF is so called biological amplification factor, which is 2.5 ± 0.7 for SCC and 1.4 ± 0.4 for BCC (*de Gruijl* and *van der Leun*, 1993). On the basis of Eq. 3, it is straightforward to derive the theoretical absolute increase of the carcinomas as a function of the latitude

$$\Delta I(\theta) = I(\theta_{ref},0) \{[(D_a(\theta,p_{eff})/D_a(\theta_{ref},0)]^{BAF} - [(D_a(\theta,0)/D_a(\theta_{ref},0)]^{BAF}\} \quad (4)$$

where θ_{ref} is the reference latitude (60 °N) and $I(\theta_{ref},0)$ is the reference cancer incidence at the reference latitude at non- depleted conditions.

Figure 20 shows a comparison of the computed annual UV-doses at vertical and horizontal surfaces as a function of the latitude. Additionally, the effect of the global depletion is shown. The calculations were carried out for clear day doses, by using the ground based total ozone data measured from 1958 to 1980 (*London*, 1985). The annual doses were corrected for the effects of clouds (*Frederick* and *Lubin*, 1988) and reflection from the snow at 60 °N and at 70 °N (*Jokela et al.*, 1993).

The main finding from Fig. 20 is the ratio of the vertical to the horizontal dose, which is 0.35 at the equator and increases to 0.5 at 60 ºN. This is mainly due to the relative increase of the diffuse radiation from the sky and ground compared with the direct radiation from the sun. The relative increase of the vertical dose at high latitudes may have some influence on the biological amplification factors which are based on epidemiological data and horizontal doses. However, the horizontal doses decrease more steeply as a function of latitude than the vertical doses which are more relevant for the facial exposure. When the BAF for SCC is derived on the basis of vertical doses it increases from 2.5 to 3.2. It is interesting that the increased BAF is closer to the murine BAF, which varies from 3.2 to 4.4 (*de Gruijl* and *van der Leun*, 1993).

Table 4 shows the effective decrease of the total ozone, the increase of annual UV-dose and increase of carcinoma incidences. Figure 20 gives the theoretical absolute increase of SCCs by using the age adjusted incidence 7.1/100000/y. (7.1 cases in one year in the population of 100 000 persons). This is the cancer incidence for the males in the Finnish population in 1986 (*Finnish Cancer Registry*, 1990). For the females the age adjusted incidence is 4.1. It was assumed that the ozone depletion has no contribution in these incidences, which is justified, since the latency time of the carcinomas are in general over 10 years and the major decrease of ozone has occurred only from the beginning of the eighties. The computed increases of carcinomas are maximal increases expected to occur several years after the UV has reached the maximum level in the turn of the century.

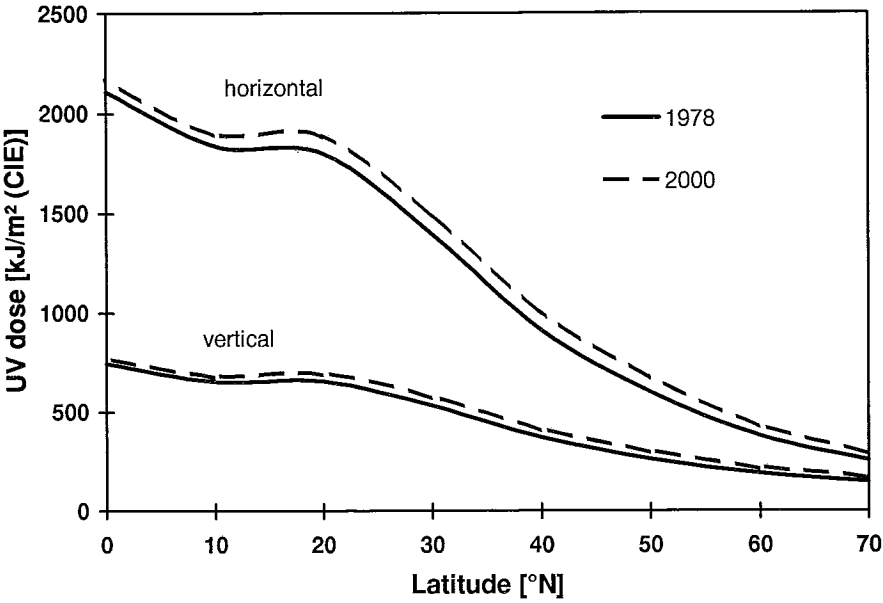

Fig. 20. Average annual clear-sky UV dose falling to vertical and horizontal surfaces at different latitudes.

Table 4. Computed fractional decrease of effective total ozone, increase of annual UV-dose (CIE) and increase of incidence of skin carcinomas. The error estimates are standard errors.

Latitude ºN	Effective decrease of total ozone, %	Increase of annual UV dose, %	Increase of BCC incidence, %	Increase of SCC incidence, %
70	-11.0 ± 3.3	12.5 ± 4.2	17.9 ± 8.3	34.2 ± 17.0
60	-10.0 ± 3.9	12.0 ± 5.2	17.2 ± 9.3	32.8 ± 19.0
50	-9.5 ± 2.6	11.9 ± 3.6	17.0 ± 7.4	32.4 ± 15.0
40	-7.5 ± 3.1	9.5 ± 4.3	13.6 ± 7.6	25.6 ± 15.0
30	-5.4 ± 3.4	6.8 ± 4.7	9.7 ± 7.3	18.0 ± 14.0
20	-3.6 ± 2.8	4.5 ± 3.7	6.4 ± 5.6	11.7 ± 10.0
10	-2.3 ± 2.5	2.9 ± 3.3	4.0 ± 4.8	7.3 ± 8.8
0	-1.9 ± 2.5	2.4 ± 3.2	3.4 ± 4.7	6.1 ± 8.7

Table 4 indicates that the fractional change of the total ozone increases from the equator toward the north being about -10% at the 60 ºN latitude. The corresponding increases in the erythemal UV-dose, BCC incidence and SCC incidence are about 12%, 17% and 33%, respectively. It is interesting to compare these values to the values interpolated from Table 1 of *Madronich* and *de Gruijl* (1994) for the 60 ºN latitude. They computed that from 1979 to 1992 the fractional increase was 7.4% for the erythemal dose, 14.1% for the BCC incidence and 26.6 % for the SCC incidence. By accounting the shorter time span these figures are in good agreement with the updated figures given by this study.

Figure 21 indicates that the maximal increase of the absolute incidence of the skin carcinomas occurs at the latitude of about 20 ºN although the maximal fractional (percentage) change increases monotonically towards the north. This is due to the increase of the baseline incidence towards the equator. Only very near to the equator, the decrease of the ozone depletion overcomes the effect of the high baseline skin cancer rate. One must strongly emphasise that the incidence increase given by Eq. 4 is only the theoretical increase of a hypothetical population transferred from the reference latitude to latitude þ. Additionally, it must be assumed that the clothing and outdoor activities of the population does not change, not always a realistic assumption when comparing the possibilities to solar UV exposure in cold and warm climates.

The main obstacle preventing the quantitative risk analysis of for the malignant skin melanoma is the lack of the relevant data of the action spectrum for the melanoma. Moreover, the relationship between the exposure and skin cancer is more complicated than in the case of the skin carcinomas, and there may be also other significant risk factors not related to the UV radiation. At the moment the best guess is, that the 10% decrease of the total ozone results in an increase of the malignant skin melanoma varying from 0 to 34%.

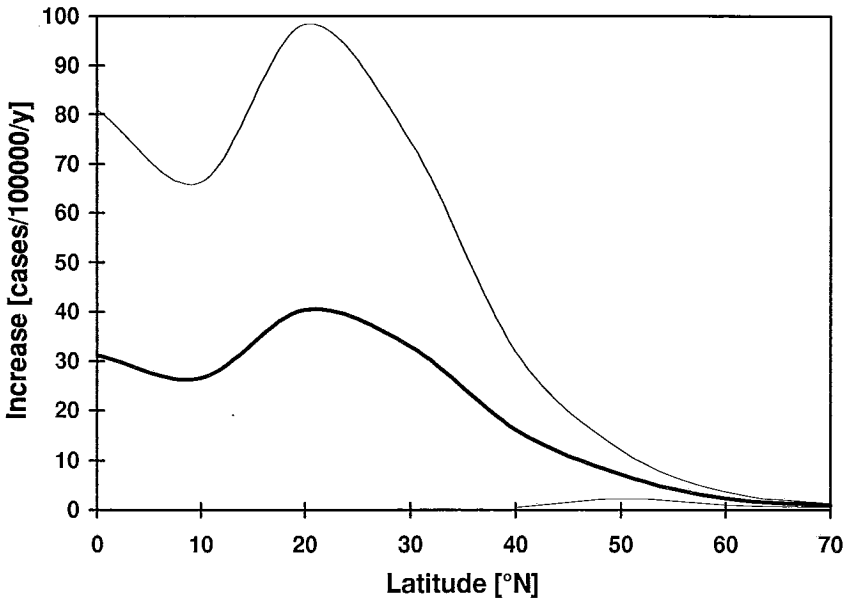

Fig. 21. Absolute increase of the skin cancer (SCC) as a function of the latitude for a hypothetical population where the age adjusted skin cancer incidence is 7.1/100000/y in normal ozone conditions. The reference latitude is 60 ºN. The thin lines denote standard errors.

In summary, the erythemally effective biological doses are relevant also for skin carcinomas. The maximal depletion of the total ozone at about 60th latitude is - 12%.

The corresponding fractional increases of annual UV doses, basal cell cancers and squamous cell cancers are 12%, 17% and 33%, respectively. For melanoma no well established estimates can be given. When the facial exposure is determined on the basis of the vertical exposure, the biological amplification factor of the SCC are in a better agreement with the results given by mice experiment.

10. Summary and conclusions

Ozone and UV radiation research have become an important part of Finnish environmental research during recent years due to the fact that largest negative trend in stratospheric ozone in the Northern Hemisphere has been detected at the latitudes of Finland. This may have led to noticeable enhancement of solar UV-B radiation. Three groups have formed the core of this research: FMI Sodankylä Observatory, STUK Laboratory for non-ionizing radiation and FMI Section of ozone and UV research. These groups have been working under Finnish national climate research programme, SILMU during 1990-95.

Classically climatologists have been using ground-based observations of temperature for studying climate change. From meteorological point of view observations made in the free atmosphere rather than in the boundary layer would be more useful for detecting possible climate change. In practice lack of long-term reliable radiosounding records with global coverage is a big problem. In this study more than three decades of homogenised temperature soundings have been used. A warming up to 0.3 K/decade during 1958-94 in the lower and middle troposphere has been found. In the lower stratosphere a cooling trend of the order of -0.3 K/decade has been found. This negative trend has been most pronounced during the winter months, which may have led to more ozone loss-favouring stratospheric climate in the European Arctic. This finding suggests a need for additional studies of large-scale lower stratospheric climatic change as a possible contribution to observed negative trends in stratospheric ozone.

The Finnish records of total ozone and vertical distribution of ozone are too short for trend analysis. In case of total ozone it is possible to extend the Brewer record of Sodankylä (starting 1988) by adding TOMS satellite observations made for Sodankylä (starting 1978). By this way we have found negative trends of total ozone for 1979-94 at Sodankylä (1979-88 TOMS, 1988-94 Brewer), i.e. -8.0 ± 3.4%/decade for winter, -3.2 ± 1.5%/decade for summer, and -4.1 ± 1.2%/decade for autumn. The Sodankylä ozone sounding record (1988-) is the longest available in the European Arctic. The ozone sounding records are especially valuable for studying the climate forcing of tropospheric ozone. The sign of this forcing depends on the trends of upper tropospheric ozone. This study of tropospheric ozone changes for 1989-94 has revealed a negative "trend" of the order of -2%/year. Longer records are needed to confirm the direction of tropospheric ozone change.

The studies of Antarctic ozone "hole" have led to largely accepted consensus about its chemical background. In the Arctic the picture is more unclear. This is due to more unstable and warmer polar vortex. The observations of Arctic winter/springtime stratospheric chemistry suggest e.g. less complete dehydration and denitrification, as compared with Antarctica. Although the heterogeneous processes related to PSCs are not completely understood, we have studied the backgrounds of observed ozone anomalies during 1989-95 in the European Arctic by using 50 hPa temperature as an explaining parameter. It has been observed that majority of the ozone anomalies detected in that region are linked to "warm" 50 hPa temperatures. This is a considerable difference with regards to the Antarctic ozone loss morphology. Nevertheless, also indications of possibly chemically induced ozone loss in the Arctic winter/spring have been found, especially in 1995.

The world-wide studies of solar UV irradiance are strongly suffering from accurate instruments. Therefore every UV measurement effort has to include high-level testing and calibration facilities. In this work the broadband UV radiometers of FMI have been characterised, tested and recalibrated by STUK. This work has also included definition of curves for correcting UV records. The UV spectroradiometers of FMI, the one of STUK have participated in NOGIC-93 UV and ozone instrument intercomparison, and the Jokioinen spectroradiometer in the European Ispra intercomparison in 1995. Also an international WMO/STUK broadband instrument intercomparison was carried out in 1995. These efforts are made to minimise the errors of UV measurements.

In this study the effect of ozone loss on UV doses have been studied. It has been found out that the effect of ozone loss may be detected from the UV observations. It has been estimated from observations and model calculations that cloudiness is absorbing about 40% of the UV radiation on annual mean basis. It has been shown, that theoretically the snowcover may intensify the UV irradiance considerably especially on a vertical surface, like human face or eyes. In this study it has been calculated that the 12% ozone loss at 60 °N may lead to 17-33 % increase in at least non-melanoma skin cancers in Finland during next few decades.

Additional efforts are needed to fully understand the behaviour of stratospheric ozone in the Northern Hemisphere. The new generation of satellites that are able to measure the vertical distribution of Clx, Brx, NOy, HOx, Ozone and aerosols, like UARS, ADEOS, ODIN, ENVISAT-1 and METOP-1 will be of importance for these studies, as well as long-term monitoring of these species by using ground-based instruments. These data are also needed to further develop the models simulating stratospheric chemistry and dynamics. To fully understand the global behaviour of tropospheric and lower stratospheric ozone and their impact on climate additional ozone sounding stations are needed. IGBP-IGAC project ITOY (International Tropospheric Ozone Years) is designed to solve this problem. FMI has active role in all of the above mentioned activities.

UV radiation research is also strongly in an evolving phase. The means to further improve the accuracy of UV instruments and data correction methods are currently developed as part of European (EU) and world-wide (WMO) activities. The past, present and future behaviour of UV radiation in the Arctic will be intensively studied during 1996-99 as part of EU Environment and Climate Programme.

The future development of stratospheric ozone and UV radiation in the Arctic depends on the success in reduction of the halogenated compound emissions and on climatic change. Increase of atmospheric CO_2 concentration may change stratospheric climate in the Arctic towards ozone-loss favouring direction with increases in UV-B irradiances.

Acknowledgements

The FMI scientists acknowledge Director-General Erkki Jatila for the initiatives and support to Finnish ozone and UV research. The installation and maintenance work performed by the staffs of Technical Department and the Jokioinen Observatory, especially Antti Aarva, Asko Tuominen and Esa Saarinen has been very important for this research. Reijo Visuri and Lasse Ylianttila from the STUK are acknowledged for their contributions on this study. Dr. Arne Dahlback and Dr. Arve Kylling are acknowledged for their modelling work. We thank Dr. Ann Webb, University of Manchester, and Dr. Mario Blumthaler, University of Innsbruck, for kindly giving a permission to use their spectral measurements for the development of the RS-correction method. We also acknowledge the technical support received by Dr. Foeke Kuik, KNMI, for the calibration of the Brewer spectroradiometer. The results shown in this study have been largely funded by the SILMU Programme of Finnish Academy. Financial support by the Nessling's Foundation, the Nordic Council of the Ministers and Ministry for the Environment in Finland is also acknowledged. This study has also been partly related to the EASOE and SESAME campaigns, funded by the CEC Environment and Climate Programme.

References

Akimoto, H., Nakane, N., and Matsumoto, Y., 1994. The chemistry of oxidant generation: Tropospheric ozone increase in Japan, In: The Chemistry of the atmosphere: Its impact on Global Change, J.G. Calvert (Ed.), Blackwell Sci. Publ., Oxford, 261-273.

Austin, J., N. Butchart and K.P. Shine, 1992. Possibility of an Arctic ozone hole in a doubled-CO2 climate. *Nature* **360**, 221-225.

Austin, J. and N. Butchart, 1994. The influence of climate change and the timing of stratospheric warmings on Arctic ozone depletion. *J. Geophys. Res.* **D99**, 1127-1145.

Bojkov, R.D., 1988. Ozone variations in the Northern polar region. *Meteorol. Atmos. Phys.* **38**, 117-130.

Braathen, G.O., M. Rummukainen, E. Kyrö, U. Schmidt, A. Dahlback, T. Jörgensen, R. Fabian, V. Rudakov, M. Gil and R. Borchers, 1994. Temporal development of ozone within the arctic vortex during the winter of 1991/92. *Geophys. Res. Lett.*, **21**, 1407-1410.

Bird, R.E. and C. Riordan, 1986. Simple solar spectral model for direct and diffuse irradiance on horizontal and tilted planes at the earth's surface for cloudless atmospheres. *Journal of Climate and Applied Meteorology,* **25**, 97-97.

Blumthaler, M. and W. Ambach, 1988. Solar UVB-albedo of various surfaces, *Photochem. and Photobiol.*, **48**, 85-88.

Dahlback, A. and K. Stamnes, 1991. A new spherical model for computing the radiation field available for photolysis and heating at twilight. *Planet. Space Sci.*, **39**, 671-683.

EN-SCI Corporation, 1994, Instruction Manual for Model Z ECC-O3-Sondes, 21 p.

Farman, J.C., B.G. Gardiner and J.D. Shanklin, 1985. Large losses of total ozone in the Antarctica reveal seasonal ClOx/NOx interaction. *Nature,* **315**, 207-210.

Von der Gathen, P., M. Rex, N.R.P. Harris, D. Lucic, B.M. Knudsen, G.O. Braathen, H. De Backer, R. Fabian, H. Fast, M. Gil, E. Kyrö, I.S. Mikkelsen, M. Rummukainen, J. Staehelin and C. Varotsos, 1995. Observational evidence for chemical ozone depletion over the Arctic in winter 1991-92. *Nature,* **375**, 131-134.

De Gruijl, F.R. and J.C. van der Leun, 1994. Estimate of the wavelength dependency of ultraviolet carcinogenesis in humans and its relevance to the risk assessment of a stratospheric ozone depletion. *Health Phys.*, **67**, 319-325.

De Gruijl, F.R. and J.C. van der Leun, 1993. Influence of ozone depletion on the incidence of skin cancer - Quantitative prediction, In: Young, A.R., L.O. Björn, J.M. Moan and W. Nultsch: Environmental UV Photobiology, Plenum Press, New York and London.

Finnish Cancer Registry, 1990. Cancer incidents in Finland 1986, Cancer statistics of the National Board of Health, Helsinki 1990.

Frederick, J.E. and D. Lubin, 1988. The budget of biologically active ultraviolet radiation in the earth-atmosphere system. *J. Geophys. Res.*, **93**, 3826-3832.

Gaffen, D., Effects of changes in radiosonde instruments and practices on climatological upper-air temperature records. *WMO Instruments and Observing Methods Report* No. **57**, 1994.

Gardiner, B.G. and P.J. Kirsch, 1995. Intercomparison of Ultraviolet Spectro-radiometers. Ispra, 24-25 May 1995, Draft Report, 127 p.

Green, R.E., K.R. Cross and L.A. Smith, 1980. Improved analytic characterisation of ultraviolet skylight. *Photocem. and Photobiol,*. **31**, 59-65.

Huovila, S. and A. Tuominen, 1990. On the influence of radiosonde lag errors on upper-air climatological data in Finland 1951-1988. *Meteorological Publications* No. **14**, Finnish Meteorological Institute, Helsinki.

Isaksen, I.S.A. and F. Stordal, 1986. Antarctic ozone depletion: 2-D model studies. *Geophys. Res. Lett.*, **13:12**, 1327-1330.

Isaksen, I.S.A., B. Rognerud, F. Stordal, M.T. Coffey and W.G. Mankin, 1990. Studies of Arctic Stratospheric Ozone in a 2-D model including some effects of zonal asymmetries. *Geophys. Res. Lett.*, **17:4**, 557-560.

Isaksen, I., E. Kyrö, T. Laurila, P. Taalas, T.S. Jörgensen, L.P. Riishöjgaard, F. Stordal, Ö. Hov and L. Zetterberg, 1995. Ozone as a climate gas, NMR Environmental Research Programme, Final Report.

Jokela, K., K. Leszczynski and R. Visuri, 1993. Effects of arctic ozone depletion and of snow on UV exposure in Finland. *Photocem. and Photobiol.*, **58**, 559-566.

Jokela, K., K. Leszczynski, R. Visuri and L. Ylianttila, 1995. Increased UV exposure in Finland in 1993. *Photocem. and Photobiol.*, **62**, 101-107.

Knudsen, B., P. von der Gathen, G.O. Braathen, R. Fabian, T.S. Jörgensen, E. Kyrö, R. Neuber and M. Rummukainen, 1994. Temporal Development of the Correlation Between Ozone and Potential Vorticity in the Arctic in the Winters of 1988/89, 1989/90 and 1990/91, In: Ozone in the Troposphere and Stratosphere, Ed. R.D. Hudson, (Quadrennial Ozone Symposium, 1992), *NASA Conference Publication* **3266**, 504-507.

Koskela, T., P. Taalas and K. Leszczynski, 1994. Correction method for Robertson-Berger type ultraviolet radiometer data, Preprints 8th Conference on Atmospheric Radiation, 23 - 28 January, 1994, Nashville, Tennessee, USA, pp. 161-163.

Kyrö, E., P. Taalas, T.S. Jörgensen, B. Knudsen, F. Stordal, G. Braathen, A. Dahlback, R. Neuber B.C. Kruger, V. Dorokhov, V.A. Yushkov, V.V. Rudakov and A. Torres, 1992. Analysis of the ozone soundings made during the first quarter of 1989 in the Arctic. *J. Geophys. Res.*, **97**, 8083- 8091.

Kyrö, E., 1993. Intercomparison of total ozone data from Nimbus 7 TOMS, UV-spectrophotometer Brewer and a UV-visible spectrophotometer SAOZ at high latitude observatory Sodankylä. *Geophys. Res. Letters*, **20**, 571-574.

Leszczynski K., 1996. UV monitoring in Finland: past, present and future. In: B.L. Diffey (Ed.), Measurement & trends of terrestrial UVB radiation in Europe, Organizzazione Editoriale Medico Farmaceutica, Milan, in press.

Leszczynski, K., K. Jokela, R. Visuri and L. Ylianttila, 1996. Calibration of the broadband radiometers of the Finnish solar UV monitoring network. *Metrologia*, Vol **32**, in press.

Leszczynski, K., K. Jokela, R. Visuri, L. Huurto, J. Simola, T. Koskela, P. Taalas and A. Aarva, 1993. Performance tests of two Robertson-Berger type UV meters solar light model 500 and 501. In: K. Stamnes (Ed.), *Atmospheric Radiation, Proc.*, Vol *2049*, pp. 162-173.

Logan, J.A., 1994. Trends in the vertical distribution of ozone: An analysis of ozonesonde data. *J. Geophys. Res.*, **99**, 25553-25585.

London, J., 1985. The observed distribution of atmospheric ozone and its variations, In: Ozone in Free Atmospheric (edited by R.C. Whitten and S.S. Prasad), Van Nostrand Reinhold Company, New York, 11-80.

Longstreth, L.D., F.R. de Gruijl, M.L. Kripke, Y. Takizawa and J.C. van der Leun, 1995. Effects of increased solar ultraviolet radiation on human health. *Ambio*, **24**, 153-165.

Lunelund, H. & K.T. Holmberg, 1929. Uber die ultraviolette Sonnenstrahlung in Finnland Commentationes Physico-Mathematicae V. 2. R. Friedlander & Sohn, Berlin, 41 p.

Lunelund, H., 1944. Starke der ultravioletten Sonnenstrahlung in Finnland, Commentationes Physico-Mathematicae XII. 13. Centraltryckeriet, Helsinki, 21 p.

Madronich, S. and F.R. de Gruijl, 1994. Stratospheric ozone depletion between 1979 and 1992: Implications for biologically active ultraviolet-B radiation and non-melanoma skin cancer incidence. *Photocem. and Photobiol.* **59**, 541-546.

McKinley, A.F. and B.L. Diffey, 1987. A reference action spectrum for ultraviolet induced erythema in human skin. *CIE-Journal*, **6**, 17-22.

Mikkelsen, I.S., B. Knudsen, E. Kyrö and M. Rummukainen, 1994. Tropospheric ozone over Finland and Greenland, 1988-94. Danish Meteorological Institute, Scientific report 94-4.

Oltmans, S.J., 1993. Climatology of Arctic and Antarctic tropospheric ozone. In: Tropospheric Chemistry of Ozone in the Polar Regions, H. Niki and K.H. Becker (Eds.), Springer-Verlag, Berlin Heidelberg, 25-40.

Pawson, S., B. Naujokat and K. Labitzke, 1995. On the PSC formation potential of the Northern stratosphere. *J. Geophys. Res.*, in press.

Prather, M., M.M. Garcia, R. Suozzo and D. Rind, 1990. Global Impact of the Antarctic Ozone Hole: Dynamical Dilution With a Three-Dimensional Chemical Transport Model. *J. Geophys. Res.*, **95**, 3449-3471.

Rex, M., P. von der Gathen, N.R.P. Harris, E. Reimer, A. Beck, R. Alfier, B.M. Knudsen, I.S. Mikkelsen, M.P. Chipperfield, D. Lucic, M. Allaart, H. DeBacker, G.O. Braathen, S. Reid, H. Claude, F. O'Connor, H. Dier, H. Fast, A. Gamma, M. Gil, S. Godin, M. Guirlet, E. Kyrö, M. Rummukainen, Z. Litynska, B. Kois, G. Murphy, F. Ravegnani, C. Varotsos, J. Wenger, V. Yushkov, V. Dorokhov, C. Zerefos, D. Balis and I. Ziomas, 1995. Chemical ozone loss in the Arctic winters 1991/92 and 1994/95 (MATCH), Third European Symposium on Polar Stratospheric Ozone Research, Schliersee, 18-22 September 1995.

Rind, D., R. Suozzo, N.K. Balachandran, A. Lacis and G. Russell, 1988. The GISS Global Climate-Middle Atmosphere Model. Part I: Model Structure and Climatology. *J. Atm. Sci.*, **45**, 329-370.

Rosenfield, J.E., P.A. Newman and M.R. Schoeberl, 1994. Computations of diabatic descent in the stratospheric polar vortex. *J. Geophys. Res.*, **99**, 16677-16689.

Rummukainen, M., T. Laurila and R. Kivi, 1996. Yearly cycle of lower tropospheric ozone at the Arctic Circle. *Atm. Env.*, **30**, in press.

Schothorst, A., H. Slaper, D. Telgt, B. Alhadi and D. Suurmond, 1987. Amounts of ultraviolet B (UVB) received from sunlight or artificial UV sources by various population groups in the Netherlands. In: Human Exposure to Ultraviolet Radiation, Risks and Regulations (edited by W.F. Passchier and B.F.M. Bosnjakovic), Excerpta Medica, Amsterdam, 269-273.

Sliney, H.D., 1986. Physical factors in cataractogenesis: Ambient ultraviolet radiation and temperature. *Investigative Ophthalmology & Visual Science*, **27**, 781- 790.

Sliney, H.D., 1994. Dosimetry for ultraviolet radiation exposure of the eye. Proc. Ultraviolet Radiation Hazards SPIE- The International Society for Optical Engineering, SPIE Vol. 2134B, 26-27 January 1994, Los Angeles.

Stein, B., 1995. PSCs and Aerosols: Ground-based measurements. Third European Symposium on Polar Stratospheric Ozone Research, Schliersee, 18-22 September 1995.

Stein, B., F. Immler, R. Kivi, E. Kyrö, B. Mielke, V. Mitev, P. Rairoux, V. Rizi, L. Stefanutti, C. Wedekind and L. Wäste, 1995. Observations of stratospheric aerosols by multispectral 2-polarization lidar. European Aerosol Conference, September 18-22, 1995, Helsinki, Finland.

Stordal, F., I.S.A. Isaksen and K. Horntvedt, 1985. A diabatic two-dimensional model with photochemistry: Simulations of ozone and long-lived tracers with surface sources. *J. Geophys. Res.*, **90**, 5757-5776.

Strahan, S.E., J.E. Rosenfield, M. Loewenstein, J.R. Podolske and A.J. Weaver, 1994. Evolution of the 1991-92 Arctic vortex and comparison with the Geophysical Fluid Dynamics Laboratory SKYHI general circulation model. *J. Geophys. Res.*, **99**, 20713-20723.

Taalas, P., 1993. Factors affecting the behaviour of tropospheric and stratospheric ozone in the European Arctic and in Antarctica. *Finnish Meteorological Institute, Contributions* No. **10**, 138 p.

Taalas, P., E. Kyrö, A. Supperi, V. Tafuri and M. Ginzburg, 1993. Vertical distribution of tropospheric ozone in Antarctica and in the European Arctic. *Tellus*, **45B**, 106-119.

Taalas, P. and E. Kyrö, 1994. The stratospheric winter 1991/92 at Sodankylä in the European Arctic with respect to 1965-1992 meteorological and 1988-92 ozone sounding statistics. *Geophys. Res. Lett.*, **21**, 1207-1210.

Taalas, P., J. Damski, A. Korpela, T. Koskela, E. Kyrö and G. Braathen, 1995. Connections between atmospheric ozone, the climate system and UV-B radiation in the Arctic. In: Wang, W.C. and I.S.A. Isaksen (Eds.): Ozone as a climate gas. Springer-Verlag, Heidelberg, *Nato ASI Series* Vol. **32**, 411-426.

Taalas, P., J. Damski, E. Kyrö, M. Ginzburg and G. Talamoni, 1996. The Effect of Stratospheric Ozone Variations on UV-radiation and on Tropospheric Ozone at High Latitudes. *Journal of Geophysical Research*, in press.

Taalas, P., 1996. On the morphology of stratospheric ozone anomalies in the European Arctic 1989-95. Submitted to *Geophysical Research Letters*.

Tabazadeh, A., R.P. Turco, K. Drdla, M.Z. Jacobson, and O.B. Toon, 1994. *Geophys. Res. Lett.*, **21**, 1619-1622.

Tarasick, D.W., D.I. Wardle, J.B. Kerr, J.J. Bellefleur and J. Davies, 1995. Tropospheric ozone trends over Canada: 1980-199?. *Geophys. Res. Lett.*, **22**, 409-412.

WMO, 1985. Atmospheric Ozone 1985, World Meteorological Organization, Global Ozone and Monitoring Project-Report No. 16.

WMO, 1991. Scientific Assessment of Ozone Depletion: 1991. World Meteorological Organisation, Global Ozone Research and Monitoring Project, Report no. 25.

WMO, Scientific Assessment of Ozone Depletion 1994, 1994, World Meteorological Organization, Global Ozone Research and Monitoring Project, Report No. 37.